crystals

MDPI

Article

Influences of Munsell Neutral Gray Backgrounds and Illuminants on Green Nephrite Color and Its Color Clustering Characteristics

Qingfeng Zhu and Nai Wang *

School of Gemmology, China University of Geosciences, Beijing 100083, China; cugbzqf@126.com
* Correspondence: 2003011807@cugb.edu.cn

Abstract

To explore the color features of Russian green nephrite (locally named "Bi Yu" in the Chinese gem trade), specimens with continuous color gradients were analyzed using XRF, UV–Vis spectroscopy, *CIE 1976 L*a*b** color measurement, controlled illuminant and background tests, cluster analysis, and discriminant analysis. This work investigates the coloring mechanism and proposes an exploratory, data-driven color classification scheme. XRF results reveal that the overall concentration of chromophore elements in Russian green nephrite is relatively low. Its green hue may stem from the combined influences of Fe, Cr, Mn, and Ni. UV–Vis spectroscopic measurements reveal characteristic absorption bands near 660 nm and 690 nm, which correspond to the electron transitions $^4A_{2g}$ (F) → $^2T_{1g}$ (G) and $^4A_{2g}$ (F) → ^4E_g(G). Such absorption signatures are consistent with the Cr^{3+} coloration system widely reported for green jadeite. Quantitative colorimetric data indicate that the chroma C^* of Russian green nephrite is co-determined by the red–green axis a^* and yellow–blue axis b^*, among which b^* serves as the core parameter governing color saturation. The hue angle $h°$ shows barely any systematic variation with a^* or b^*, suggesting weak linear correlations. Illuminant A tends to decrease the green component and chroma of green nephrite and may lead to inconsistent color evaluation. D65, as a CIE standard daylight illuminant, tends to better resolve intrinsic color variations with relatively higher chroma, favoring the discrimination of subtle color differences between samples. D50 yields visually comparable hues and could act as an alternative daylight reference when D65 is inaccessible, although its lower chroma limits its ability to distinguish fine color disparities. Under the Munsell N9 neutral gray background, D65 appears favorable as the reference illuminant for the quantitative color assessment of Russian green nephrite. The chroma C^* of green nephrite tends to increase and the hue angle $h°$ tends to decrease as the luminance factor of Munsell neutral gray backgrounds rises. Higher chroma benefits the discrimination of subtle color variations. Among the tested gray substrates, Munsell N9 produces relatively high chroma for Russian green nephrite, indicating its potential suitability as the background for color assessment of these samples. Combined cluster and discriminant analyses based on colorimetric parameters were used to explore the classification of the 20 Russian green nephrite samples into three color groups exhibiting statistically significant inter-group differences. This study characterizes the color-modulating effects of Munsell neutral gray backgrounds and standard illuminants, and provides experimental data and an exploratory color classification scheme for Russian green nephrite, a scheme that requires further validation using independent samples.

Keywords: Russian green nephrite; light source; Munsell background; color clustering

Check for updates

Academic Editor: Vladislav V. Gurzhiy

Received: 23 September 2026
Revised: 10 November 2026
Accepted: 14 November 2026
Published: 17 November 2026

Copyright: © 2026 by the authors. Licensee MDPI, Basel, Switzerland. This article is an open access article distributed under the terms and conditions of the Creative Commons Attribution (CC BY) license.

1. Introduction

Since ancient times, nephrite has been widely cherished by the Chinese people, as its soft luster, glossy color, compact and delicate texture, and mild, understated sheen perfectly conform to the aesthetic preferences of the Chinese nation. From a mineralogical perspective, nephrite consists mainly of amphibole minerals of the tremolite–actinolite isomorphic series, characterized by extensive isomorphic substitution between magnesium and iron. Based on the grain size, morphology, and intergranular bonding pattern of constituent mineral particles, nephrite mainly develops a felt-like interwoven blastic texture, a microfibrous blastic texture, and a microfibrous cryptocrystalline texture [1]. This unique mineral texture endows nephrite with a fine, mild, greasy luster. In terms of color appearance, nephrite exhibits a diverse range of color varieties, predominantly including "Bai Yu", "Qing Bai Yu", "Qing Yu", "Cui Qing Yu", "Bi Yu", "Mo Yu", and "Tang Yu" [2,3]. Among them, "Bi Yu" (green nephrite) refers to a type of nephrite whose body generally exhibits various hues ranging from light green to dark green, including grayish green, bluish green and faint yellowish green; its coloration is attributed to trace elements such as Fe, Ni, Cr, and Ti [3,4].

As the dominant variety of nephrite in the gem and jewelry market, green nephrite features diverse color tones, fine texture, and a mild, glossy appearance, rendering it highly valuable for jade carving, jewelry fabrication, and antique collecting. Its color acts as a core index for quality classification, commercial pricing, and visual aesthetic assessment. The primary provenances of green nephrite include Xinjiang [5], Canada [6], Qinghai [7], New Zealand [8], Australia [9], and other regions. In the traditional evaluation system of jade, the color judgment of green nephrite mainly relies on the subjective visual experience of practitioners, a practice accompanied by prominent subjectivity, randomness, and individual discrepancies. Without unified, standardized quantitative evaluation criteria, inconsistent color assessment results and disordered grading standards frequently arise for the same specimen under different observation environments. This issue severely restricts the establishment and optimization of standardized identification and grading systems for green nephrite.

With the rapid advancement of gem colorimetry, the *CIE1976 L*a*b** color space has emerged as a mainstream technique for the quantitative characterization of gemstones, owing to its perceptual uniformity and independent parameters for lightness, hue, and chroma [10]. This method has been successfully applied to garnet [11], jadeite [12], and other gem varieties.

Unlike traditional qualitative visual description, the *CIE 1976 L*a*b** color space precisely quantifies the lightness, hue, and chroma of green nephrite through three core coordinate parameters: lightness L*, the red–green parameter a*, and the yellow–blue parameter b*. It transforms the color evaluation of green nephrite from subjective textual description into objective numerical quantification, thereby providing a scientific foundation for the standardized color assessment of this material.

Existing academic research on green nephrite mainly focuses on its geochemical characteristics [13], origin and processing technology [14], spectroscopic properties [15–17], gemological features [18], mineralogical properties [19–21], color-forming elements [5,22], microstructures [23,24], metallogenic genesis [25,26], and provenance discrimination [27,28]. For Russian green nephrite, however, quantitative colorimetric characterization and color parameter analysis remain insufficient. In particular, few studies have systematically investigated the dynamic variation patterns of its color coordinates under different external observation environments.

The visually perceived color of jade cannot fully reflect the intrinsic mineral properties; instead, it is a visual result jointly determined by the inherent color characteristics of the

specimen and by observational conditions, including illumination sources and viewing backgrounds. External observation environments constitute the primary extrinsic factor triggering visual color deviations in gemstones. As a prerequisite for color perception, standard illuminants with distinct spectral power distributions directly alter the color rendering of objects. Meanwhile, the lightness gradient of viewing backgrounds alters human color perception through visual contrast effects.

In this study, Russian green nephrite specimens covering a continuous range of hue and lightness values were selected as study materials. Based on the *CIE 1976 L*a*b** color space, precise measurements were carried out to acquire the *L**, *a**, *b** coordinate data of the samples under three standard illuminants (D50, D65, and A) and nine grades of Munsell neutral gray backgrounds (N1–N9).

This quantitative analysis examines how chromatic features and background gray levels affect the color appearance of Russian green nephrite, and further reveals the color deviation mechanism of this material under various observation environments. It establishes standardized specifications for observational environments applicable to commercial inspection and laboratory research, offering scientific colorimetric support for accurate color grading, unified identification, and quality evaluation of Russian green nephrite. Additionally, the findings can serve as a reference for environment-adaptive color assessment of other green gem varieties.

2. Materials and Methods

2.1. Materials

A total of 20 Russian green nephrite specimens were selected for this experiment. All specimens were uniformly cut into square tiles of 10 mm × 10 mm × 4 mm and numbered sequentially from HJ-1 to HJ-20. The specimens exhibit distinct gradients in hue, lightness, and chroma, forming a continuously varying green series from light green to dark green.

Black mineral inclusions, color bands, and uneven color distribution were observed in some specimens. The specimens display a vitreous luster, with transparency ranging from translucent to opaque, and their specific gravity varies between 2.97 and 3.01. The samples are shown in Figure 1. The samples were purchased from commercial gem rough suppliers. Only the country of origin (Russia) could be confirmed; the specific mine or deposit could not be traced. This study focuses on color quantification and classification of green nephrite rather than mine-specific provenance research.

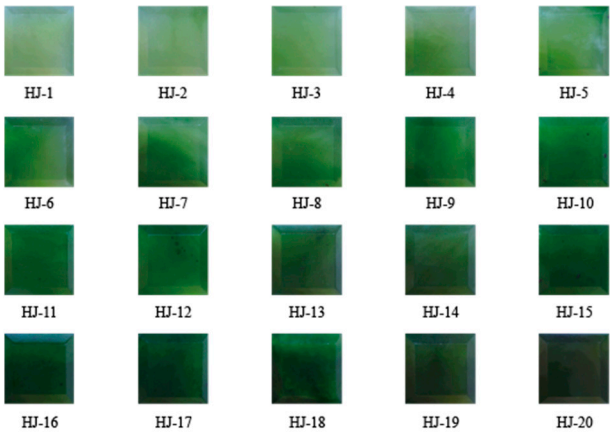


Figure 1. The 20 green nephrite samples.

2.2. Methods

2.2.1. UV–Vis Absorption Spectral Analysis

The UV–Vis optical absorption spectra were acquired on a UV 3600 spectrophotometer (Shimadzu, Tokyo, Japan) over the 300–800 nm range in specular reflection mode. Measurements were performed at a medium scan speed, with a sampling interval of 1.0 nm and a time constant of 0.1 s. The light-source switching wavelength was set to 300.00 nm, whereas the detector and grating switching wavelengths were both set to 850 nm, with S/R reversed.

2.2.2. Energy-Dispersive X-Ray Fluorescence Analysis

EDXRF analysis of the green nephrite chemical composition was carried out at the Gem Identification Laboratory, School of Gemmology, China University of Geosciences (Beijing, China), on an EDX-7000 energy-dispersive X-ray fluorescence spectrometer (Shimadzu, Tokyo, Japan). The measurement parameters were set as follows: for the Ti–U range, 50 kV, acquisition range 0–40, collimator aperture 4.00–35.00, and testing duration 60 s; for the Al–Sc range, 15 kV, acquisition range 0–20, collimator aperture 0.00–4.40, and testing duration 60 s; and for the S–Ca range, 15 kV, acquisition range 0–20, No. 2 collimator with an aperture of 10–4.10, and testing duration 60 s.

2.2.3. Colorimetric Parameter Testing

Color parameters of the 20 green nephrite specimens were collected using an X-Rite SP64 portable spectrophotometer (X-Rite, Grand Rapids, MI, USA). Measurements were taken at the center of each sample, targeting clean, uniform areas with a 4 mm aperture, under the D65 illuminant. Spectral data were recorded in reflectance mode with the 2° standard observer, covering the wavelength range of 400–700 nm, while specular reflectance was excluded.

Color results for each sample were averaged over three replicate readings. The Munsell neutral gray scale comprises gray patches graded from 0.5 to 9.5 with a 0.25 unit interval, and it serves broadly in instrument calibration, image evaluation, and reflectance reference applications. In this experiment, nine glossy Munsell neutral gray backgrounds from N1 to N9 were adopted as viewing substrates. Three standard illuminants were utilized throughout the experiment, namely Illuminant A (CCT 2856 K), D65 (CCT 6504 K), and D50 (CCT 5003 K). The color data under different standard illuminants were obtained by computational conversion from measured reflectance spectra, rather than direct physical measurement under separate lighting sources.

2.2.4. *CIE (1976) L*a*b** Uniform Color Space System

Officially recommended by the CIE, the *CIE 1976 L*a*b** uniform color space serves as a standard tool for quantitative color characterization. It forms a three-dimensional coordinate system defined by the vertical lightness axis L^* and the two in-plane chromatic axes a^* and b^*. The L^* parameter represents lightness with a scale ranging from 0 to 100, corresponding to pure black and pure white at the two endpoints. The chromatic coordinate a^* describes the red–green opposition: positive values correspond to red, and negative values to green. The chromatic coordinate b^* characterizes the yellow–blue opposition, where positive values correspond to yellow and negative values to blue. Chroma C^*_{ab} represents the color's chroma, while the hue angle h°_{ab} represents the counterclockwise angle from the $+a^*$ axis to the (a^*, b^*) color vector and is used to indicate the hue. The chroma C^*_{ab} and hue angle h°_{ab} are calculated from a^* and b^* using the quadrant-corrected Equations (1) and (2).

$$C^*_{ab} = [(a^*)^2 + (b^*)^2]^{1/2} \quad (1)$$

$$h^{\circ}_{ab} = arctan2(b^*, a^*) \quad (2)$$

For nephrite specimens, color differences induced by changes in illuminants and backgrounds were quantified using the *CIEDE2000* (ΔE_{00}) formula. Compared with the conventional CIELAB (ΔE*ab) color difference formula, this model delivers superior perceptual uniformity that better matches human visual perception. In this formula, $\Delta L'$, $\Delta C'$, and $\Delta H'$ represent the lightness difference, chroma difference, and hue difference, respectively.

The correction term R_T mitigates the interaction between hue and chroma parameters in the blue wavelength region; K_L, K_C, and K_H represent experimental calibration coefficients, with two widely recognized standard sets documented in academia: *CIEDE2000* (2:1:1) [29] and *CIEDE2000* (1:1:1) [30]. S_L, S_C, and S_H are correction functions designed to compensate for the inherent visual non-uniformity of the original *CIELAB* system. Taking human color perception into comprehensive consideration, the *CIEDE2000* model with the coefficient ratio of (1:1:1) was selected for color difference evaluation in this study, as this parameter combination achieves higher accuracy in reproducing the visual color difference of green nephrite samples. The formula [31] is presented as follows:

$$\Delta E_{00} = \sqrt{\left(\frac{\Delta L'}{k_L S_L}\right)^2 + \left(\frac{\Delta C'}{k_C S_C}\right)^2 + \left(\frac{\Delta H'}{k_H S_H}\right)^2 + R_T\left(\frac{\Delta C'}{k_C S_C}\right)\left(\frac{\Delta H'}{k_H S_H}\right)} \quad (3)$$

3. Results and Discussion

3.1. Elemental Chemical Composition Analysis

XRF tests were performed on a set of 20 Russian nephrite specimens with continuously gradient colors. As shown in the Table 1, nephrite is dominated by SiO_2, MgO, and CaO. SiO_2 accounts for 56–60% of the total mass and serves as the primary constituent. Minor color-forming oxides including Fe_2O_3, Cr_2O_3, MnO, and NiO are also detected. Among the chromogenic ions, Fe^{2+} and Ni^{2+} contribute green hues, Mn^{2+} produces pale pink tones, and Cr^{3+} imparts green color in nephrite.

Table 1. XRF chemical compositions of investigated green nephrite (wt%).

Sample	SiO_2	MgO	CaO	Fe_2O_3	NiO	MnO	Cr_2O_3	K_2O	Total
HJ-1	57.93	22.18	15.28	4.34	0.14	0.12	0.02	0.00	100.00
HJ-2	57.80	23.14	14.79	4.03	0.10	0.11	0.03	0.00	100.00
HJ-3	57.72	22.37	15.10	4.54	0.10	0.12	0.05	0.00	100.00
HJ-4	58.09	22.14	14.92	4.49	0.17	0.16	0.03	0.00	100.00
HJ-5	56.80	23.04	15.36	4.48	0.13	0.14	0.05	0.00	100.00
HJ-6	59.95	20.36	14.48	4.92	0.14	0.11	0.06	0.00	100.00
HJ-7	59.07	22.79	13.96	3.72	0.14	0.13	0.19	0.00	100.00
HJ-8	56.78	21.79	15.28	5.78	0.13	0.12	0.12	0.00	100.00
HJ-9	56.94	23.21	14.85	4.50	0.22	0.11	0.11	0.06	100.00
HJ-10	57.33	22.53	15.09	4.60	0.17	0.13	0.15	0.00	100.00
HJ-11	58.32	21.45	15.04	4.81	0.20	0.07	0.12	0.00	100.00
HJ-12	56.39	22.79	15.26	4.97	0.24	0.14	0.16	0.06	100.00
HJ-13	57.93	22.03	15.00	4.73	0.13	0.08	0.10	0.00	100.00
HJ-14	57.19	22.54	15.50	4.47	0.16	0.08	0.07	0.00	100.00
HJ-15	58.08	21.25	15.10	4.77	0.29	0.11	0.41	0.00	100.00
HJ-16	56.81	21.36	15.85	5.20	0.30	0.12	0.37	0.00	100.00
HJ-17	56.99	21.95	15.61	4.62	0.26	0.10	0.47	0.00	100.00
HJ-18	56.97	22.39	15.06	4.85	0.23	0.09	0.41	0.00	100.00
HJ-19	57.44	22.41	15.17	4.56	0.19	0.07	0.11	0.06	100.00
HJ-20	57.13	21.89	15.55	4.73	0.26	0.12	0.32	0.00	100.00

A ternary diagram was plotted based on the mass fractions of Cr_2O_3, MnO, and NiO. The data points show a continuous compositional trend corresponding to the color transition of green nephrite from light green to dark green. Data points of light green specimens (HJ-1–HJ-5) cluster near the MnO vertex, featuring the highest relative proportion of MnO and a low Cr_2O_3 content. As the green chroma increases, the relative proportions of Cr_2O_3 and NiO rise simultaneously, while the proportion of MnO decreases steadily. Data points of dark green samples (HJ-16–HJ-20) lie close to the Cr_2O_3 vertex, where Cr_2O_3 reaches its maximum relative content and MnO its minimum (Figure 2).

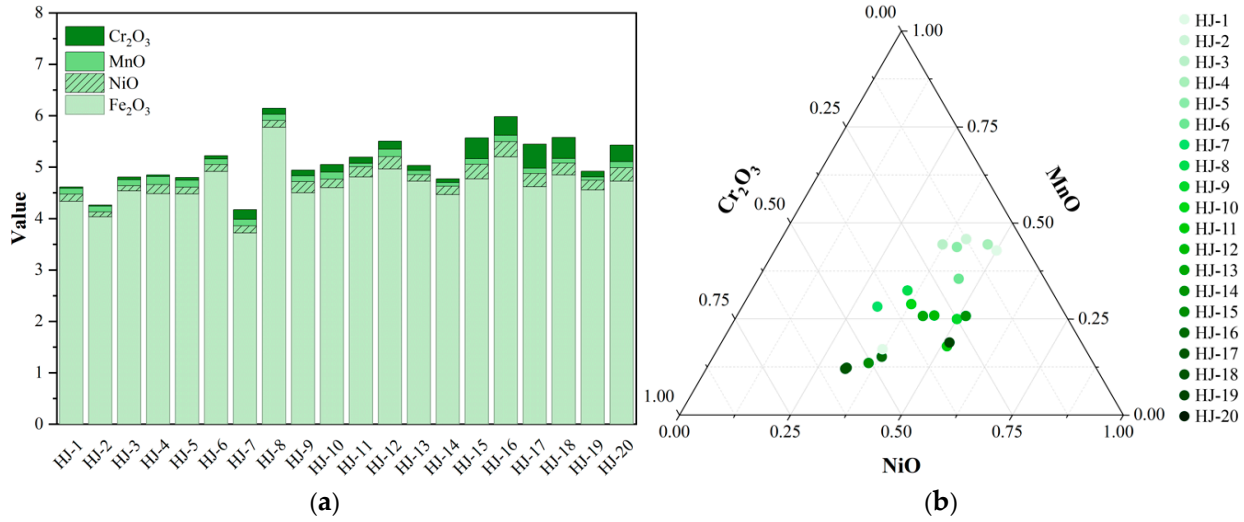


Figure 2. (**a**) Percentages of Fe, Cr_2O_3, MnO, and NiO for the investigated green nephrite. (**b**) Normalized concentrations of Cr_2O_3, MnO, and NiO for the investigated green nephrite.

Only HJ-8 has an abnormally high Fe content and intense green color, suggesting a possible correlation between Fe and green intensity. Higher Cr and Mn contents tend to correspond to deeper green, and higher Ni to lighter green. Fe, Cr, Mn, and Ni act as chromophoric elements [22]. The depth and vividness of the green color may relate to the combined effect of Cr, Mn, and Ni [32].

3.2. UV–Vis–NIR Optical Spectroscopic Analysis

Absorption spectra were collected for green nephrite specimens with varying green chroma over the 300–800 nm range, as illustrated in Figure 3. The spectral data agree well with those reported in previous studies. Three characteristic absorption features are identified in the visible region: a broad blue-violet absorption band from 420 to 520 nm containing weak absorption peaks at 445 nm and 495 nm, a broad orange-red absorption band ranging from 590 to 670 nm, and a narrow red absorption band between 680 and 710 nm. The absorbance is positively correlated with the color intensity of specimens. The spectra demonstrate strong light absorption in the blue-violet, orange, and red regions, whereas light is preferentially reflected in the yellow-green band. These spectral characteristics collectively give rise to the vivid green visual appearance of green nephrite. Based on the above results, the green color of green nephrite is mainly attributed to transition metal ions including Fe, Cr, Mn, and Ni, and the light absorption behavior of these ions forms the fundamental origin of its green hue.

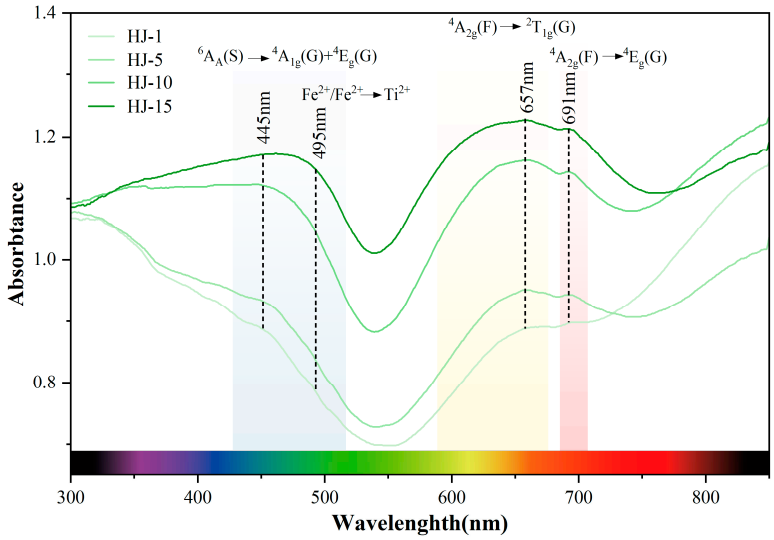


Figure 3. UV–Vis–NIR spectra of investigated green nephrite.

The absorption peak at 445 nm arises from the electron transition $^6A_{1g}(S) \rightarrow {}^4A_{1g}(G) + {}^4Eg(G)$. The absorption signal at 495 nm is ascribed to the $Fe^{2+} \rightarrow Fe^{3+}$ charge-transfer transition. In comparison, the absorption near 490 nm arises from either the $Fe^{2+} \rightarrow Ti^{4+}$ charge transfer or the spin-forbidden transitions of Cr^{3+} [33]. The absorption bands around 660 nm and 690 nm are analogous to features reported for green jadeite; they correspond to the $^4A_{2g}$ (F) $\rightarrow {}^2T_{1g}$ (G) and $^4A_{2g}$ (F) $\rightarrow {}^4E_g(G)$ electron transitions of Cr^{3+} [34].

Table 2 summarizes all UV–Vis absorption peaks detected in the specimens and their corresponding spectral assignments.

Table 2. Visible absorption of the green nephrite samples.

Wavelength (nm)	Assignment
445	The $^6A_{1g}(S) \rightarrow {}^4A_{1g}(G) + {}^4E_g(G)$ electronic transition of Fe^{3+}
495	Fe^{2+}–Fe^{3+} charge transfer
657	The $^4A_{2g}$ (F) $\rightarrow {}^2T_{1g}$ (G) electronic transition of Cr^{3+}
691	The $^4A_{2g}$ (F) $\rightarrow {}^4E_g(G)$ electronic transition of Cr^{3+}

3.3. Spectral Color Quantification of Green Nephrite

Measured under the D65 standard illuminant on a Munsell N9 neutral gray background, the color parameters of the 20 green nephrite samples with continuous color gradients spanned the following ranges: lightness L^*(14.18–47.24), red–green coordinate a^*(−20.22 to −4.55), yellow–blue coordinate b^* (5.54–22.17), chroma C^*(7.17–29.76), and hue angle $h°$ (119.69–141.21). The color appearance of the specimens ranging from pale light green to dark green conforms to these ranges. Figure 4a shows the three-dimensional projection of color parameters acquired from the 20 samples.

As illustrated in Figure 4b,c, the color-parameter analysis of the 20 specimens shows that a^* and b^* are each strongly linearly correlated with chroma C^*: C^* decreases as the a^* coordinate increases (i.e., as the color shifts toward red), whereas it increases with increasing b^*, indicating that a^* and b^* jointly control chroma. The coefficient of determination (R^2) measures how well the regression model fits the measured data, with values approaching 1 indicating a closer fit; the Pearson correlation coefficient r measures the strength of the linear relationship between two variables, with absolute values closer to 1 corresponding to stronger linearity. The correlation between C^* and b^* ($R^2 = 0.90$) is stronger than that between C^* and the a^* axis ($R^2 = 0.78$). In the *CIE 1976 L*a*b** uniform color space, the $+b^*$

axis represents the yellow component, suggesting that b^* is the main chromatic contributor to the saturation of green nephrite. The hue angle $h°$ shows little systematic variation with changes in either a^* or b^*, indicating weak correlations between $h°$ and these two coordinates. The hue angles of all samples vary within a narrow range, and all 20 specimens retain a dominant green hue with no fundamental hue shift.

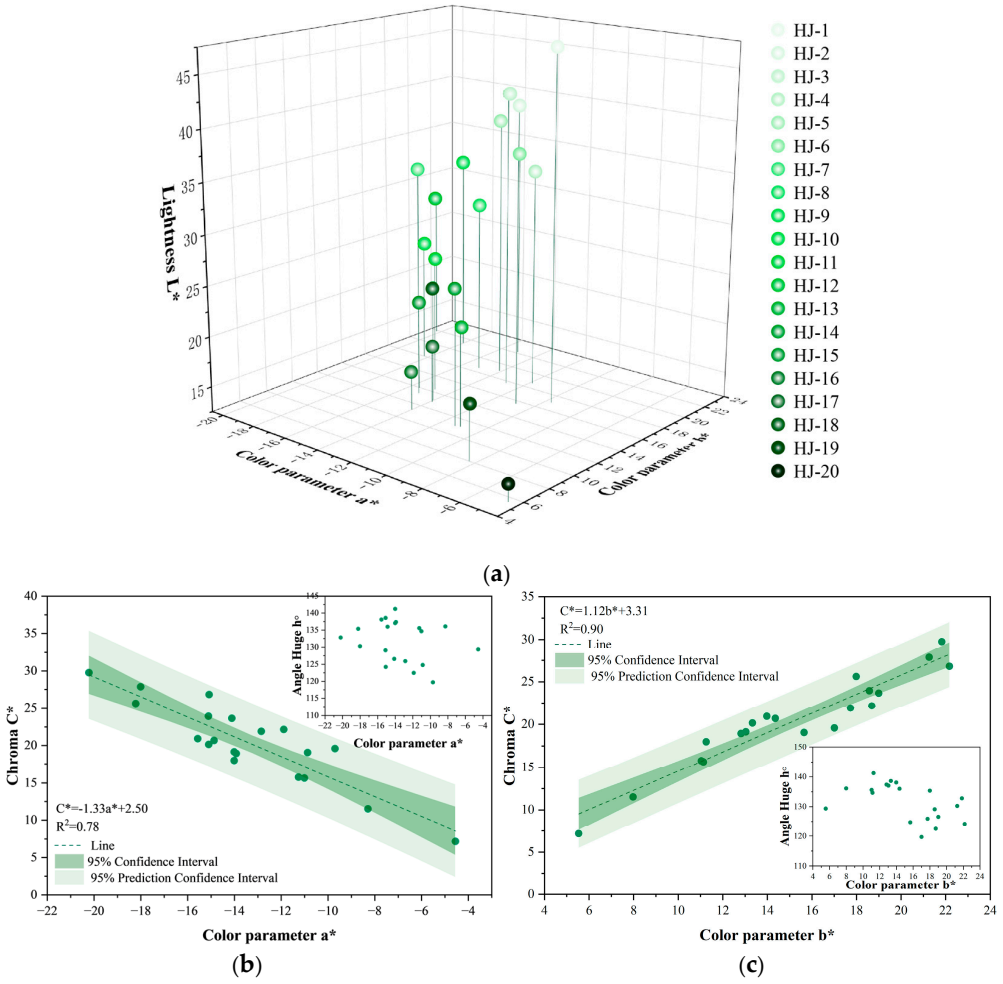


Figure 4. (**a**) Three-dimensional projection diagram of color parameters of the 20 samples. (**b**) Relationships of a^* with chroma C^* and hue angle $h°$; (**c**) relationships of b^* with chroma C^* and hue angle $h°$.

3.4. Color Variation of Green Nephrite Under Different Light Sources

Distinct discrepancies exist among various CIE standard illuminants in terms of correlated color temperature (CCT) and relative spectral power distribution (RSPD). A wide range of commonly adopted standard illuminants are available, including Illuminant A at 2856 K, fluorescent illuminants of the F series (F12 at 3000 K, F11 at 4000 K, F2 at 4230 K), as well as daylight simulators D50 (5003 K), D65 (6504 K), and D75 (7500 K). Illuminant A corresponds to conventional incandescent lamps widely used in residential and retail lighting, whose spectral energy is concentrated in the red and yellow wavelength bands. Both D50 and D65 are artificial daylight simulators with different color temperatures: D50 is primarily applied in printing platemaking and photographic imaging, while D65 reproduces the average spectral distribution of midday daylight in the Northern Hemisphere. It is widely adopted as the reference illuminant for quantitative color evaluation in many fields [35].

This study investigates the effects of three illuminants (D50, A, and D65) on the color of green nephrite against a Munsell N9 neutral gray background. Color parameter analyses were performed on 20 nephrite samples. Friedman tests with post hoc comparisons were applied for the statistical analysis of color parameters, and the results are shown in Table 3. *p*-values were used to judge the statistical significance of the effects. A result was considered statistically significant when $p < 0.05$.

Table 3. Friedman's test and post hoc comparison results under three illuminants.

	D65	A	D50	χ^2	*p*
*L**	26.79 (21.61,34.87) b	26.17 (19.84,34.33) a	26.89 (20.73,34.74) b	24.025	<0.001
*a**	−14.01 (−15.10,−11.07) b	−11.58 (−12.95,−8.86) a	−13.05 (−14.31,−10.48) a b	40	<0.001
*b**	15.01 (11.65,18.66) b	13.08 (9.45,16.23) a	14.65 (10.99,18.11) a b	40	<0.001
*C**	20.41 (18.21,23.88) b	17.32 (15.28,20.02) a	19.41 (17.13,22.63) a b	40	<0.001
h°	133.74 (126.10,136.82)	134.19 (122.61,138.06)	133.30 (124.14,136.72)	4.785	0.091

a, significantly different compared with illuminant D65; b, significantly different compared with illuminant A. Pairwise comparisons were performed with Bonferroni correction.

The medians (interquartile ranges) of the color parameters under the three illuminants were as shown in Table 3: *L**: 26.79 (21.61, 34.87), 26.17 (19.84, 34.33), 26.89 (20.73, 34.74), $\chi^2 = 24.025$, $p < 0.001$; *a**: −14.01 (−15.10, −11.07), −11.58 (−12.95, −8.86), −13.05 (−14.31, −10.48), $\chi^2 = 40$, $p < 0.001$; *b**: 15.01 (11.65, 18.66), 13.08 (9.45, 16.23), 14.65 (10.99, 18.11), $\chi^2 = 40$, $p < 0.001$; *C**: 20.41 (18.21, 23.88), 17.32 (15.28, 20.02), 19.41 (17.13, 22.63), $\chi^2 = 40$, $p < 0.001$; and *h*°: 133.74 (126.10, 136.82), 134.19 (122.61, 138.06), 133.30 (124.14, 136.72) $\chi^2 = 4.785$, $p > 0.05$. Statistically significant differences among illuminants were observed for *L**, *a**, *b**, and *C**, whereas no significant difference was found for *h*°.

Pairwise post hoc comparisons indicated statistically significant differences in *L**, *a**, *b**, *C**, and *h*° for D65 versus A and A versus D50, while no significant differences in lightness *L** and hue angle *h*° were detected between D65 and D50.

As shown in Table 4, the color shift between illuminants D65 and A was the most prominent, with ΔE_{00} ranging from 1.25 to 2.73 (mean 2.10); all twenty samples exceeded the 50:50% perceptibility threshold of $\Delta E_{00} = 0.8$ reported for dental restorative materials [36], and adopted here as an illustrative reference, and thirteen samples exceeded 2.0, suggesting a clearly perceptible color difference. In contrast, ΔE_{00} between D65 and D50 ranged from 0.35 to 1.92 (mean 0.83), with nine of the twenty samples exceeding $\Delta E_{00} = 0.8$ and the remaining eleven falling below this reference value; for most samples, color differences between these two daylight illuminants are likely to be subtle and may not be readily perceived visually. For the A–D50 pair, ΔE_{00} varied from 0.46 to 1.84 (mean 1.40), and eighteen of the twenty samples exceeded $\Delta E_{00} = 0.8$, exhibiting perceptible color differences. Overall, samples with higher chroma appeared more sensitive to illuminant variation, and their color differences were more likely to exceed the reference threshold; by comparison, dark samples with low lightness showed only minor color variation across illuminants, mostly remaining below the reference perceptibility threshold. It should be noted that the threshold used here was established for dental restorative materials rather than nephrite, and its transferability to this material is therefore not guaranteed; establishing a nephrite-specific perceptibility threshold would require dedicated psychophysical experiments.

Figure 5 shows the comparison of color parameters under illuminants D65, D50, and A. Differences in the color temperature and spectral power distribution of the illuminants affect their color-rendering properties, resulting in different color appearances of the gemstones. The perceived lightness of the samples varies with the color temperature of the illuminant. The spectral output of an illuminant varies with its correlated color temperature. The luminous flux reflected and absorbed by the sample is positively correlated with the *L**

value, leading to higher visual lightness. Even when illuminated by high-color-temperature light sources, the reflected and transmitted luminous flux of green nephrite samples remains very low due to their inherently low transparency, which greatly limits any increase in lightness (Figure 5a,d). Therefore, the L* values of the samples change only slightly when switching the illuminant from D65 to D50 and A.

Table 4. ΔE_{00} between each pair of the three lights.

Samples	D65 Simulated Color	A Simulated Color	D50 Simulated Color	ΔE_{00} (D65–A)	ΔE_{00} (D65–D50)	ΔE_{00} (A–D50)
HJ-1				2.73	1.18	1.57
HJ-2				2.14	0.88	1.31
HJ-3				2.43	0.94	1.53
HJ-4				2.51	0.89	1.66
HJ-5				2.41	0.88	1.59
HJ-6				2.40	0.88	1.55
HJ-7				2.07	0.62	1.46
HJ-8				2.14	0.76	1.41
HJ-9				2.18	0.73	1.53
HJ-10				2.05	0.53	1.62
HJ-11				1.70	0.42	1.32
HJ-12				2.25	0.78	1.55
HJ-13				1.86	0.99	1.79
HJ-14				2.36	0.55	1.84
HJ-15				1.83	1.44	0.46
HJ-16				1.74	0.62	1.41
HJ-17				1.98	0.49	1.55
HJ-18				2.52	1.92	1.20
HJ-19				1.25	0.35	0.98
HJ-20				1.54	0.79	0.78

The spectral power distribution of illuminant D65 is mainly concentrated in the blue–green region (400–550 nm), while its intensity in the red–yellow region (550–700 nm) is relatively low. Compared with D65, illuminant D50 has a slightly higher proportion of red and yellow light, though blue–green light still accounts for a certain proportion. Illuminant A is obviously biased toward the red–yellow region (600–700 nm), with almost no blue–green light. Since the color tone of the samples lies between green and yellow, their a^* values are negative and b^* values are positive. When the illuminant is changed from D65 to D50 or A, the a^* values increase, indicating a decrease in the green component Figure 5b, and the b^* values decrease. In addition, the samples show their minimum a^* values under illuminant D65, and their minimum b^* values are reached under illuminant A (Figure 5d).

Figure 5c shows that the variation trend of C^* is similar to that of b^*. The C^* values measured under illuminant D65 are the highest, and the C^* values obtained under illuminant D50 fall between the other two. This occurs because D65 is dominated by blue–green light, and the spectral reflection characteristics of green nephrite produce a stronger response to the blue–green wavebands of D65, which intensifies the green tone and raises the C^* value.

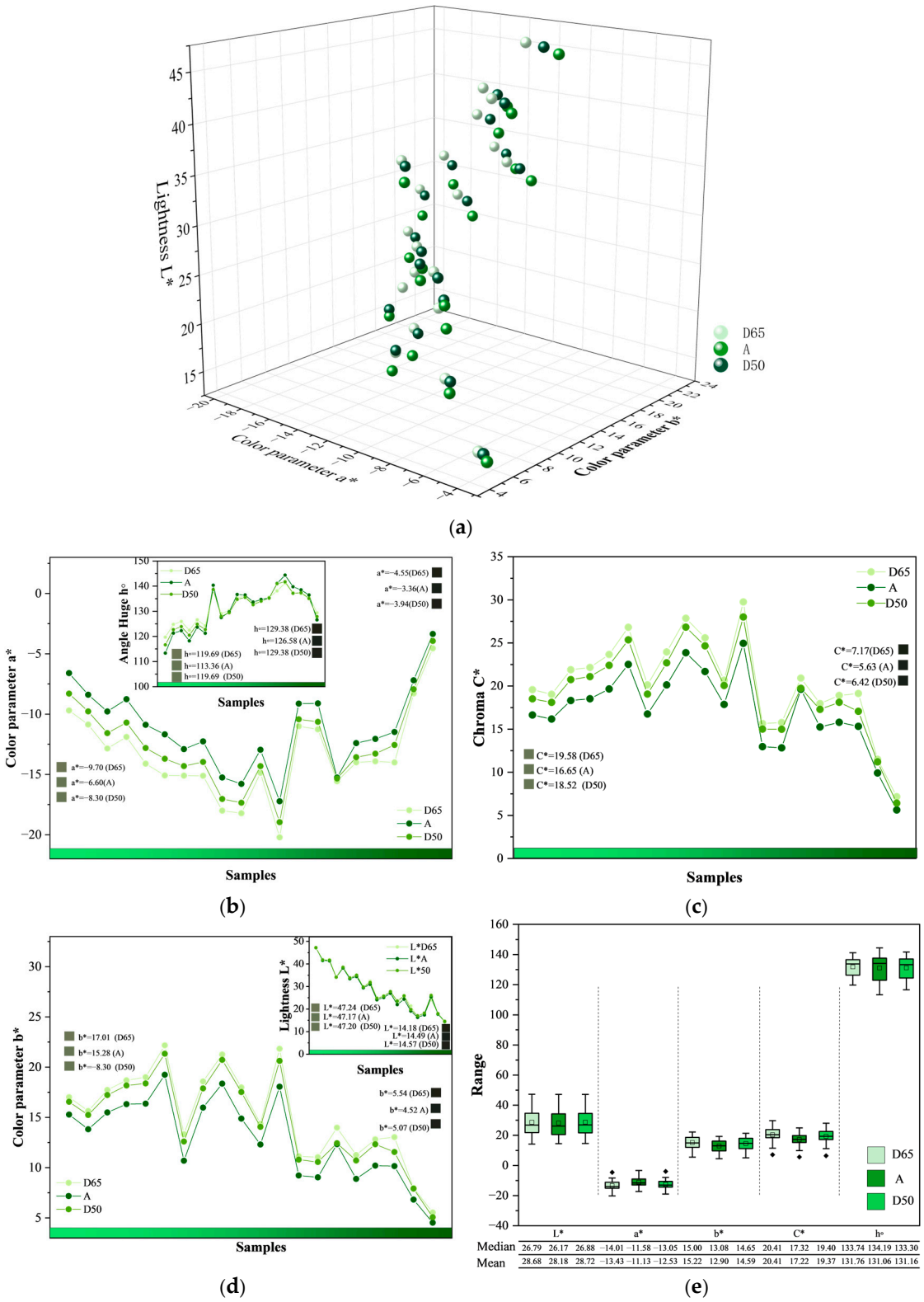


Figure 5. (**a**) Distribution in the *CIE 1976 L*a*b** color space of the samples processed with three lights. (**b**) The color parameter *a** and hue angle *h*° under three light sources. (**c**) Chroma *C** under three light sources. (**d**) The lightness *L** and the color parameter *a** under three light sources. (**e**) Boxplots of the lightness *L**, the color parameters *a**, *b**, chroma C*, and the hue angle *h*°.

Combined with the results of Friedman tests and pairwise post hoc comparisons, the illuminant exerts selective regulation on the color attributes of green nephrite. Changes in illuminant induce significant variations in *L**, *a**, *b**, and *C**, while no statistically significant

difference is found for the hue angle $h°$ between D65 and D50. Further *CIEDE2000* color-difference analysis confirms that the color shift between D65 and A is the most prominent. All the samples exhibit color differences perceptible to the human eye ($\Delta E_{00} > 0.8$) between these two illuminants. Under illuminants A and D50, the color differences of most samples exceeded the perceptibility threshold. In contrast, the color differences of most nephrite samples between D65 and D50 are difficult to resolve visually.

Illuminant A systematically reduces the green component and chroma of green nephrite, which tends to yield unstable grading results and is therefore unsuitable for color grading of this type of green nephrite. As the CIE standard daylight illuminant, D65 can fully reveal the inherent color differences among samples and produce higher chroma, facilitating the identification of subtle color distinctions between specimens. D50 produces hues that are visually indistinguishable from those under D65 for most samples, and can therefore serve as an alternative daylight reference when D65 is unavailable. Nevertheless, the overall chroma under D50 is lower, and its capacity to discriminate minor color differences is weakened. In summary, under the condition of the Munsell N9 neutral gray background, D65 is preferred as the reference illuminant for quantitative color grading of Russian green nephrite.

3.5. Color Variation of Green Nephrite Under Different Backgrounds

Owing to the intrinsic luster and transparency of green nephrite, changing Munsell neutral gray backgrounds with different lightness levels substantially alters its perceived color appearance [37]. The observed color changes mainly originate from the optical effects introduced by the Munsell neutral gray backing, rather than visual surround effects. Accordingly, all measurements in this study were performed under the D65 standard illuminant. Using an X-Rite SP64 portable spectrophotometer, the color parameters of 20 green nephrite samples were measured across nine Munsell neutral gray backgrounds ranging from N1 to N9. Table 5 presents how specimen color varies with the observation substrate, summarizes the average color values of nephrite under the nine Munsell neutral gray backgrounds, and quantifies the color difference between every pair of gray substrates.

The Munsell neutral gray system is divided into 37 lightness gradients covering a lightness range of 0 to 100, labeled from N0.5 to N9.5 with an interval of 0.25 lightness units between adjacent grades. Each gray grade corresponds to a unique background luminance factor (γb). The correlation between the background luminance factor γb of Munsell neutral substrates and substrate lightness L_b* is expressed as follows:

$$L_b^* = 116\gamma_b^{1/3} - 16 \quad (4)$$

Color mixing can be categorized into two mechanisms: additive mixing and subtractive mixing. Additive mixing produces new colors by projecting and superimposing multiple light beams with distinct spectral power distributions; the total lightness of the mixed light rises synchronously as the intensity of each monochromatic light increases. Subtractive mixing generates color through the superposition of multiple colored media, which act as spectral filters [38]. Figure 6c illustrates that the lightness of specimens increases as background lightness increases. The relationship between specimen lightness L^* and γ_b is obtained by fitting the Munsell neutral background luminance factor against specimen lightness, which is expressed as follows:

$$L^* = 6.62\gamma_b + 24.11\left(R^2 = 0.96\right) \quad (5)$$

Table 5. Variation of green nephrite color parameters across Munsell neutral backgrounds.

Background		**N1**	**N2**	**N3**	**N4**	**N5**	**N6**	**N7**	**N8**	**N9**
γ_b		0.0121	0.03126	0.06555	0.12000	0.19770	0.30050	0.43060	0.59100	0.78660
L^*_b		10.63	20.56	30.76	41.22	51.58	61.70	71.60	81.35	91.08
Photos										
Color parameters	L^*	23.77	24.49	24.43	24.80	25.65	26.44	27.26	28.45	28.68
	a^*	−11.97	−11.85	−11.99	−12.07	−12.03	−12.00	−11.91	−12.56	−13.43
	b^*	11.65	11.74	11.74	11.84	12.02	12.35	12.71	13.21	15.22
ΔE_{00}	N1	-	-	-	-	-	-	-	-	-
	N2	0.54	-	-	-	-	-	-	-	-
	N3	0.48	0.12	-	-	-	-	-	-	-
	N4	0.76	0.28	0.28	-	-	-	-	-	-
	N5	1.39	0.87	0.91	0.63	-	-	-	-	-
	N6	2.00	1.48	1.53	1.26	0.62	-	-	-	-
	N7	2.66	2.13	2.18	1.92	1.29	0.66	-	-	-
	N8	3.60	3.09	3.12	2.85	2.23	1.62	1.04	-	-
	N9	4.25	3.79	3.81	3.55	3.01	2.47	1.97	1.23	-

The semi-transparent property of green nephrite is the core reason that its lightness varies with background lightness. A higher background lightness leads to greater luminous flux transmitted through or reflected by the nephrite matrix, which ultimately manifests as a corresponding increase in the overall lightness of the specimens. Figure 6b shows the trends of green nephrite chroma C^* and hue angle $h°$ against background grayness: chroma C^* rises consistently with increasing background lightness, while the hue angle $h°$ decreases gradually. Separate regression fits of chroma and hue angle against the Munsell neutral background luminance factor γ_b yield the following functional relationships:

$$C^* = 3.74\gamma_b + 16.48 \ (R^2 = 0.77) \quad (6)$$

$$h° = -5.39\gamma_b + 136.62 \ (R^2 = 0.88) \quad (7)$$

Unlike the correlation between nephrite lightness and background lightness, the effect of different neutral gray backgrounds on nephrite chromaticity does not follow the rule of subtractive color mixing, as neutral backgrounds carry no chromatic components. As shown in Figure 6d, chroma C^* exhibits a distinct linear correlation with chromatic coordinates a^* and b^*. In the *CIE 1976 L*a*b** color space, the positive b* axis represents yellow tones while the negative a* axis corresponds to green tones. This implies that the chroma of green nephrite is mainly determined by these yellow and green color components. Given that the yellow hue possesses the highest lightness, the chromatic coordinate b^* of specimens rises as background lightness increases, whereas the chromatic coordinate a^* declines accordingly. This trend is illustrated in Figure 6a. As a result, the color data points gradually shift toward the positive b^* axis alongside a decrease in hue angle $h°$, as demonstrated in Figure 6d.

Based on the fitted relationships between the luminance factor of Munsell neutral backgrounds and the color parameters of green nephrite, specimen chroma C^* increases with a rising background luminance factor, while hue angle $h°$ gradually decreases. The higher chroma helps discriminate subtle color differences among green nephrite samples. Within the range of neutral gray substrates tested in this study, the Munsell N9 background

yields relatively higher chroma values for the measured Russian green nephrite. This suggests that N9 may be a favorable background for the color assessment of these specimens.

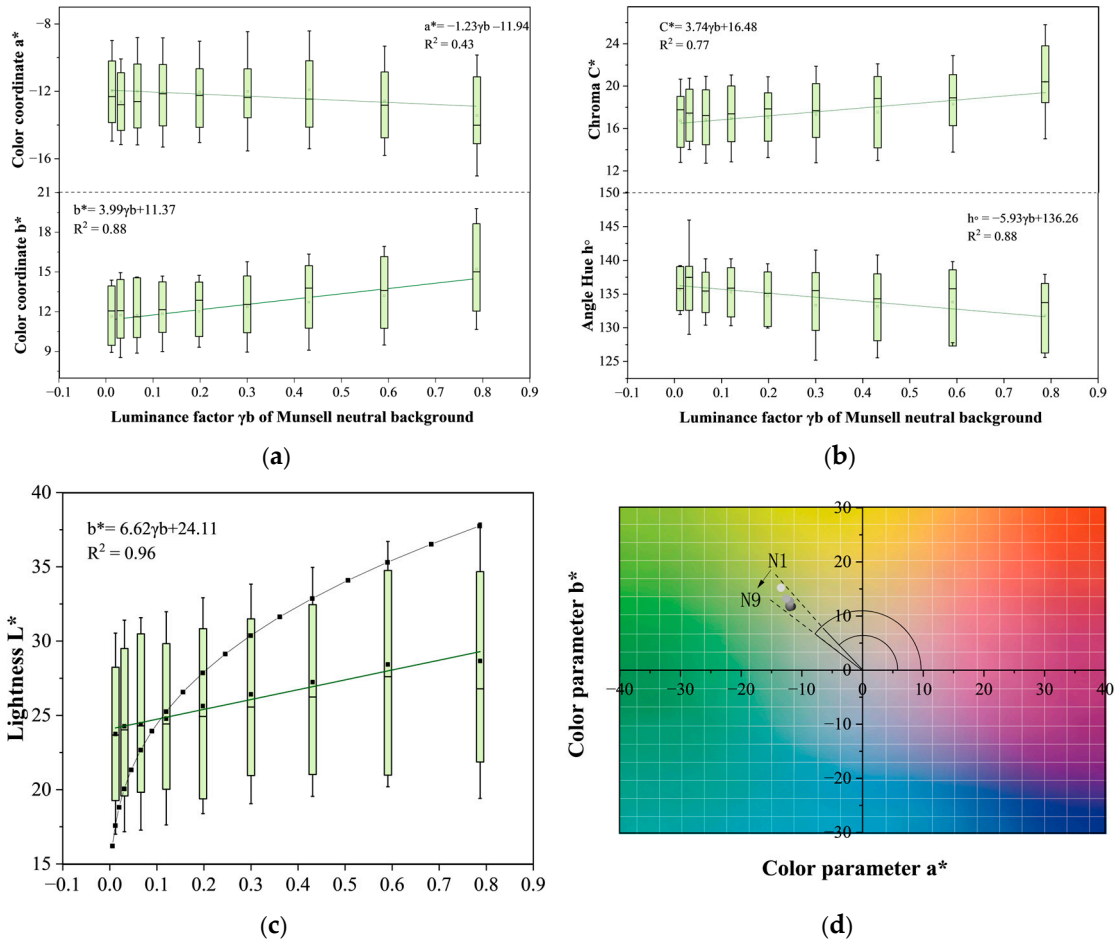


Figure 6. Variation of the Munsell neutral background under D65 illumination alters the perceived color of specimens. (**a**) Boxplots of a^*, b^*, and γ_b; (**b**) boxplots of C^*, $h°$, and γ_b; (**c**) boxplots of sample lightness L^* together with background lightness versus γ_b; (**d**) correlation between a^* and b^* across different backgrounds.

3.6. Clustering Analysis of Color Parameters

Clustering is an exploratory data analysis technique designed to uncover latent grouping structures within datasets. It categorizes specimens based on their inherent attributes: samples with highly similar features are assigned to the same cluster, enabling objective data stratification and revealing hidden distribution patterns and correlations embedded in the data. The classic K-means clustering algorithm iteratively solves for cluster centroids to minimize the total distance from all samples to their respective cluster centers [39]. This work applies K-means clustering coupled with Fisher discriminant analysis for quantitative assessment of the color features of green nephrite. The Fisher discriminant analysis in this study serves only as internal validation of the cluster classification, not as independent cross-validation. Future work will introduce an independent sample set for external validation.

The K-means clustering algorithm implemented in SPSS 29.0.10.0 (171) was used in this work. Three color indicators from the *CIE 1976 L*a*b** uniform color space, namely lightness L^*, the red–green coordinate a^*, and the yellow–blue coordinate b^*, were used as input variables to group the 20 green nephrite specimens by color. To ensure objectivity and comparability of the experimental results, all color measurements were performed

under fixed observation conditions—a Munsell N9 neutral gray background and the D65 light source—and the clustering analyses were based on these measurements. Silhouette scores were calculated for K = 2, 3, and 4 (Table 6). This range was chosen on the basis of the typical number of color grades adopted in the commercial grading of green nephrite. The highest silhouette score was observed at K = 2. Although this value indicates the best mathematical separation into two clusters, a two-category division is inadequate for the practical color grading of green nephrite. Therefore, K = 3 was adopted as an exploratory grouping scheme, and Fisher discriminant analysis was applied as an internal consistency check of this three-group partition rather than as an independent validation. The differences among the three groups were statistically significant (Sig < 0.01). The color differences among the three groups exceed the illustrative reference value of $\Delta E_{00} = 0.8$ [36], indicating that the inter-group color differences are likely to be visually distinguishable. The sample sizes of the three clusters are 4, 8, and 8, respectively. The clustering results are summarized in Table 7, and the cluster centroids are listed in Table 8. Fisher discriminant analysis was then applied to examine the internal consistency of the partition; the resulting in-sample classification accuracy indicates that the three clusters are well separated in the measured color space, but this result does not constitute independent validation of the grouping scheme. Accordingly, the three-cluster solution should be regarded as exploratory, and its robustness should be tested on independent samples in future work. The corresponding discriminant functions are given below:

$$F_1 = 2.734L^* - 1.355a^* + 0.246b^* - 69.178 \quad (8)$$

$$F_2 = 1.397L^* - 1.554a^* - 0.257b^* - 22.718 \quad (9)$$

$$F_3 = 1.944L^* - 1.623a^* + 0.461b^* - 48.017 \quad (10)$$

Table 6. Silhouette scores for K = 2, 3, and 4.

Number of Clusters	2	3	4
Silhouette scores	0.532	0.478	0.472

Table 7. Cluster analysis results of green nephrite.

Color Parameter	Clustering		Error		F	*p*
	Mean Square	Df	Mean Square	Df		
*L**	683.959	2	15.566	17	43.940	<0.001
*a**	46.237	2	8.996	17	5.140	<0.018
*b**	129.209	2	8.083	17	15.986	<0.001

Referring to China's National Standard GB/T 23885-2009 for jadeite [40], which categorizes gem color based on hue, chroma, and value, green nephrite specimens with hue angles ranging from 119.69° to 141.21° are classified into three categories: (1) Light Green, (2) Green, and (3) Deep Green. It is worth noting that this study only draws on the standard's color classification framework rather than adopting its original jadeite grading thresholds. The hue interval boundaries were reconstructed using measured color parameters of nephrite samples through K-means clustering and Fisher discriminant analysis to fit the characteristics of Russian green nephrite.

- Grade I (Green): Specimens with relatively high lightness L^* (24.9–35.07), moderate-to-high chroma C^* (20.14–29.76), and hue angles $h°$ ranging from 122.47° to 138.58°. This type of nephrite exhibits an intense, saturated green appearance with strong color saturation and commands relatively high market value.

- Grade II (Light Green): Specimens with medium lightness L^* (38.49–47.24), medium chroma C^* (19.05–23.66), and hue angles $h°$ shifted toward yellowish (119.69–126.59°).
- Grade III (Deep Green): Specimens with low lightness L^* (14.18–25.97), relatively low chroma C^* (7.17–20.92), and hue angle $h°$ range (129.38–141.21°). This grade features a dark, deep green appearance and represents the most prevalent category in commercial trading.

Table 8. Clustering center and color differences (ΔE_{00}) among different groups.

Classification	1	2	3
Cluster Center	$L^* = 42.35$ a* = −11.88 $b^* = 17.35$	$L^* = 20.06$ $a^* = -11.58$ $b^* = 10.85$	$L^* = 30.47$ $a^* = -16.06$ $b^* = 18.53$
Simulated Color			
Quantity	4	8	8
ΔE_{00}	1	2	3
1	–	17.94	10.34
2	17.94	–	9.03
3	10.34	9.03	–

To more clearly illustrate the grouping results, the distribution of the groups based on chroma and brightness as parameter values is shown in Figure 7.

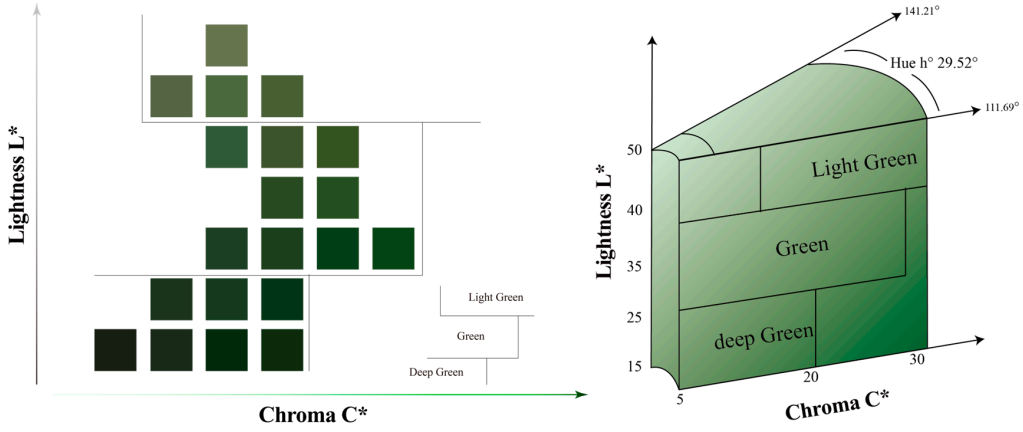


Figure 7. The color clustering of green nephrite according to L* and C*. Samples are assigned to three color grades. The coordinate axis range of this figure is non-uniform scale, aiming to optimize the visualization effect to highlight the classification boundaries.

4. Conclusions

The visual color characteristics of Russian green nephrite are jointly determined by its internal chemical composition and external viewing conditions. Iron, chromium, manganese, and nickel are the main transition-metal chromophoric ions in green nephrite. Its green color may arise from the combined effects of Fe, Cr, Mn, and Ni.

Illuminant A tends to decrease the green component and chroma of green nephrite and may lead to inconsistent color evaluation. D65, a CIE standard daylight illuminant,

tends to show sample color differences more clearly with higher chroma. D50 produces visually comparable hues and may serve as an alternative daylight reference, though its relatively lower chroma could limit the discrimination of subtle color differences. Under the Munsell N9 neutral gray background, D65 appears to be a suitable reference illuminant for the quantitative color assessment of Russian green nephrite.

Fitting results show that the specimen chroma C^* tends to rise and hue angle h° tends to fall as the luminance factor of the Munsell neutral gray background increases. Since higher chroma facilitates discrimination of subtle color differences, N9, the brightest neutral gray substrate tested in this work, produces relatively elevated chroma for the studied Russian green nephrite. Accordingly, N9 appears suitable as a background for color assessment of these samples within the experimental conditions of this study.

Combined statistical methods of cluster analysis and discriminant analysis were used to explore the classification of green nephrite specimens into three characteristic color groups: Light Green, Green, and Deep Green. This exploratory quantitative classification scheme may provide preliminary data support for constructing a standardized and reproducible color grading system for green nephrite, although further validation on independent samples is required.

Author Contributions: Conceptualization, Q.Z. and N.W.; methodology, Q.Z. and N.W.; software, Q.Z.; validation, Q.Z. and N.W.; formal analysis, Q.Z. and N.W.; investigation, Q.Z. and N.W.; resources, Q.Z. and N.W.; data curation, Q.Z.; writing—original draft preparation, Q.Z.; writing—review and editing, Q.Z.; visualization, Q.Z.; supervision, Q.Z. and N.W.; project administration, Q.Z. and N.W.; funding acquisition, Q.Z. and N.W. All authors have read and agreed to the published version of the manuscript.

Funding: This research was funded by the Fundamental Research Funds for the Central Universities, grant number 2-9-2024-061.

Data Availability Statement: The raw data supporting the conclusions of this article will be made available by the authors on request.

Acknowledgments: The authors thank the Lab of Gemmology, School of Gemmology, China University of Geosciences, Beijing, for support.

Conflicts of Interest: The authors declare no conflicts of interest.

Abbreviations

The following abbreviations are used in this manuscript:

L^*	Lightness
a^*	Color parameter a^*
b^*	Color parameter b^*
C^*	Chroma C^*
h°	Hue angle h°

References

1. Shi, M. Study on Mineralogical Characteristics and Genesis of Greeen Nephrite from Xinjiang Uyghur Autonmous Region. Master's Thesis, China University of Geosciences (Beijing), Beijing, China, 2012.
2. Ren, J.H.; Shi, G.H.; Zhang, J.H.; Yuan, Y.; Gao, K.; Wang, M.L.; Li, X.L.; Long, C. Infrared Spectra of Grayish Green Nephrite and Gray: Nephrite Characteristics and Significance. *Spectrosc. Spectr. Anal.* **2019**, *39*, 772–777.
3. *GB/T 388215-2020*; Hetian Yu Testing and Classification. Inspection and Quarantine of the People's Republic of China &National Standardization Administration: Beijing, China, 2020.
4. *GB/T 44914-2024*; Hetian Yu Granding. Inspection and Quarantine of the People's Republic of China &National Standardization Administration: Beijing, China, 2024.

5. Du, H.M.; Song, J.D.; Ku, Y.M.; Wang, Y.Y. Influence of Color-causing Ion of Manas Jasper on Green Color Parameters. *Superhard Mater. Eng*. **2015**, *27*, 53–58.
6. Liu, J. A gemological study of jasper from the Cassiar mine, Canada. *Acta Petrol. Mineral*. **2014**, *33*, 10–14.
7. Zhang, H.Q. Gemology, Mineralogy and Trace Element Study on Green Nephrite from Qinghai Province. Master's Thesis, China University of Geosciences (Beijing), Beijing, China, 2019.
8. Liu, X.F.; Zhang, H.Q.; Liu, Y.; Zhang, Y.; Li, Z.J.; Zhang, J.H.; Zheng, F. Mineralogical Characteristics and Genesis of Green Nephrite from the World. *Rock Mineral. Anal*. **2018**, *37*, 479–489.
9. Zhao, X.H. Study of Gemological Mineralogy of Green Nephrite from South Australia, Australia. Master's Thesis, China University of Geosciences (Beijing), Beijing, China, 2014.
10. *CIE.ISO/CIE 11664-4:2019(E)*; Colorimetry—Part 4: CIE 1976 L*a*b* Color Space. International Organization for Standardization and International Commission on Illumination: Geneva, Switzerland, 2019.
11. Ma, Y.M.; Guo, Y. The Impact of Munsell Neutral Gray Backgrounds on Tsavorite's Color and Study on the Evaluation Method of Color Gem Cutting. *Appl. Sci*. **2023**, *13*, 1673. [CrossRef]
12. Liu, Z.Y.; Guo, Y. The Effect of Munsell Neutral Value Scale on the Color of Yellow Jadeite and Comparison between AP and K-Means Clustering Color Grading Schemes. *Crystals* **2022**, *12*, 241. [CrossRef]
13. Yu, H.Y.; Yang, X.W. Geochemical characteristics, metallogenetic resource and processes of jasper from the world's major producer. *J. Guilin Univ. Technol*. **2019**, *39*, 311–320.
14. Guo, F.X. The Manasi Green Jade in The Collection of The Qing Court during Emperor Qianlong's Regime. *J. Palace Mus*. **2015**, *2*, 6–31+157.
15. Wang, L.B.; Liu, Y.L. The X-ray powder diffraction feature of Hetian jade, Manasi green jade and Xiuyan old jade(tremolite jade). *Acta Petrol. Mineral*. **2002**, *21*, 62–67.
16. Guo, L.H.; Han, J.Y. The IR analyses of M1and M3cation occupation of Hetian jade□ Manasi green jade and Xiuyan old jade. *Acta Petrol. Mineral*. **2002**, *21*, 68–71.
17. Zou, T.R.; Guo, L.H.; Li, W.H.; Duan, Y.R. A study on Raman spectra of Hetian jade□Manasi green jade and Xiuyan old jade. *Acta Petrol. Mineral*. **2002**, *21*, 72–78.
18. Zhao, Y.Y. Study of Gemological Mineralogy of Green Nephrite from New Zealand. Master's Thesis, China University of Geosciences (Beijing), Beijing, China, 2015.
19. Sun, L.H.; Wang, S.L. Mineralogy of green nephrite jade from Canada. *Acta Petrol. Mineral*. **2014**, *33*, 28–36.
20. Zhao, Y.Y.; Wu, R.H.; Wu, Q.M.; Shi, W. A study of gemological characteristics of green nephrite in Ospa 11# mining area of Russia. *Acta Petrol. Mineral*. **2014**, *33*, 37–42.
21. Wu, Q.M.; Wu, R.H.; Zhao, Y.Y.; Shi, W. Gemological and mineralogical characteristics of green nephrite from Cassiar, Canada. *Acta Petrol. Mineral*. **2014**, *33*, 43–47.
22. Na, B.C.; Leng, Y.Y.; Li, X.H.; Shi, W. Research on coloring element of nephrite. *Superhard Mater. Eng*. **2008**, *3*, 55–58.
23. Zhang, X.Y. Gemological Characteristics of Russian Gorlik-gol Jasper and Research on Composition of Melanocratic Mineral. Master's Thesis, China University of Geosciences (Beijing), Beijing, China, 2013.
24. Shi, M.; Guo, Y. The mineralogical characteristics of jasper and the study of its scanning electron microscope. *Mineral. Depos*. **2010**, *29*, 833–834.
25. Zang, X.M. Mineralogy and Genesis of Green Nephrite in the Western Section of Manas Region, Xinjiang. Ph.D. Thesis, China University of Geosciences (Beijing), Beijing, China, 2020.
26. Ren, J.H. Mineralogy and Genesis of Green Nephrite in the Eastern Section of Manas Region, Xinjiang. Ph.D. Thesis, China University of Geosciences (Beijing), Beijing, China, 2019.
27. Liao, G.L.; Yang, X.Y.; Jing, C.; Zhou, Z.Y.; Quan, X.P. The Mineral Composition and Chemical Composition Characteristics of Green Nephrite from Three Origins. *J. Tongji Univ. (Nat. Sci.)* **2022**, *50*, 1110–1114.
28. Zhu, Y.J. Identification Characteristics of Nephrite from Different Areas. *China Gems Jades* **2020**, *3*, 73–79+54.
29. Perez, M.D.M.; Ghinea, R.; Herrera, L.J.; Ionescu, A.M.; Pomares, H.; Pulgar, R.; Paravina, R.D. Dental ceramics: A CIEDE2000 acceptability thresholds for lightness, chroma and hue differences. *J. Dent*. **2011**, *39*, e37–e44. [CrossRef]
30. Mangine, H.; Jakes, K.; Noel, C. A preliminary comparison of CIE color differences to textile color acceptability using average observers. *Color Res. Appl*. **2005**, *30*, 288–294. [CrossRef]
31. *GB/T 20147.6-2026*; Colorimetry—Part 6: CIEDE2000 Colour-Difference Formula. General Administration of Quality Supervision, Inspection and Quarantine of the People's Republic of China &National Standardization Administration: Beijing, China, 2026.
32. Han, D.; Liu, X.F.; Liu, Y.; Zhang, Y.; Zheng, F.; Maituohuti, A.; Zhang, H.Q.; Wen, Z.S. Genesis of dolomite-related nephrite from Hetian and color-forming factors of typical nephrite in Hetian, Xinjiang. *Acta Petrol. Mineral*. **2018**, *37*, 1011–1026.
33. Wang, J.X. Comparative Study of Russian and Manas Green Nephrite. Master's Thesis, China University of Geosciences (Beijing), Beijing, China, 2018.

34. Dai, L.L.; Jiang, Y.; Yang, M.X. Study on the Spectral Identification Characteristic of "Heiqing" And "Heibi". *Spectrosc. Spectr. Anal.* **2021**, *41*, 292–298.
35. Lam, Y.M.; Xin, J.H. Evaluation of the quality of different D65 simulators for visual assessment. *Color Res. Appl.* **2002**, *27*, 243–251. [CrossRef]
36. Paravina, R.D.; Ghinea, R.; Herrera, L.J.; Bona, A.D.; Igiel, C.; Linninger, M.; Sakai, M.; Takahashi, H.; Tashkandi, E.; Perez, M.D.M. Color Difference Thresholds in Dentistry. *J. Esthet. Restor. Dent.* **2015**, *27*, S1–S9. [CrossRef]
37. Jiang, Y.S.; Guo, Y.; Zhou, Y.F.; Li, X.; Liu, S.M. The effects of munsell neutral gray backgrounds on the color of chrysoprase and the application of AP clustering to chrysoprase color grading. *Minerals* **2021**, *11*, 1092.
38. Simonot, L.; Hébert, M. Between additive and subtractive color mixings: Intermediate mixing models. *J. Opt. Soc. Am. A* **2013**, *31*, 58–66. [CrossRef]
39. Coates, A.; Ng, A.Y. Learning feature representations with k-means. In *Neural Networks: Tricks of the Trade*, 2nd ed.; Montavon, G., Orr, G.B., Müller, K.R., Eds.; Lecture Notes in Computer Science 7700; Springer: Berlin/Heidelberg, Germany, 2012; ISBN 978-3-642-35288-1.
40. *GB/T 23885-2009*; Jadeite Grading. General Administration of Quality Supervision, Inspection and Quarantine of the People's Republic of China &National Standardization Administration: Beijing, China, 2009.

Disclaimer/Publisher's Note: The statements, opinions and data contained in all publications are solely those of the individual author(s) and contributor(s) and not of MDPI and/or the editor(s). MDPI and/or the editor(s) disclaim responsibility for any injury to people or property resulting from any ideas, methods, instructions or products referred to in the content.